SHOCK ADIABATS OF OXIDES OF THE ALKALINE-EARTH METALS

A. A. Vaal', A. V. Zhukov, and V. F. Konusov

UDC 539.21

The analysis of the shock adiabats of ionic crystals (alkali-halide compounds, oxides) is a necessary link in the passage to the examination of the behavior of many inorganic materials (minerals, mountain rocks) under shock compression [1-3]. The shock compression parameters of the majority of alkali-halide crystals have been determined well both experimentally [4] and theoretically [5, 6]. The behavior of oxides under shock loading conditions has been investigated much less. On the basis of a proposed semiempirical binding energy function which takes account of pairwise and triple ion interactions, the shock adiabats are analyzed in this paper for oxides of the alkaline-earth metals MgO, CaO, SrO, BaO in the phases B1 (NaCl lattice) and B2 (CsCl lattice).

The shock adiabat $P_H(V)$ is computed by means of the formula [7]

$$P_H(V)=\frac{P_x(V)+\gamma(V)\,[E_0-U(V)]/V}{1+\gamma(V)\,[V-V_0]/2V}, \tag{1}$$

where U(V), $P_x(V)$ are the energy and pressure on the zero isotherm, $\gamma(V)$ is the Gruneisen factor, and V_0, E_0 are the volume and internal energy of the free crystal. Utilization of a quantum-mechanical method of computing U(V) [5], on the basis of a pairwise approximation of the binding forces is less justified in oxides tha in alkali-halide crystals since substantial deviations from the Cauchy relationships between the second-order elastic moduli are observed there. These deviations are due primarily to three-particle interactions.

Taking account of the three-particle interactions, the crystal binding energy function formed by particles of different species has the form

$$U=\frac{1}{2}\sum_{\substack{ll'\\kk'}}\varphi(r^{ll'kk'})+\frac{1}{6}\sum_{\substack{ll'l''\\kk'k''}}\psi(r^{ll'kk'},\ r^{l''lk''k},\ r^{l''l'k''k'}), \tag{2}$$

where $r^{\varrho\varrho'kk'}$ is the spacing between particles of the species k and k' that are in the elementary cells, l and l', φ, ψ are, respectively, the potentials of the pairwise and three-particle interactions. We approximate the pairwise interaction by the Born-Maier potential

$$\varphi(r)=\frac{e_k e_{k'}}{r}+A_{kk'}\exp\left(-\frac{r}{\rho}\right)-\frac{c_{kk'}}{r^6}-\frac{d_{kk'}}{r^8},$$

where e_k, e_k' are the ion charges, $c_{kk'}$, $d_{kk'}$ are, respectively, the dipole–dipole and dipole–quadrupole interaction constants whose values for the oxides are presented in [8], and $A_{kk'}$ ρ are parameters. A potential whose functional form is proposed in [9]

$$\psi=B_{kk'k''}\exp\left(-\frac{r^{ll'kk'}+r^{l''lk''k}+r^{l'l''k'k''}}{3\rho}\right)$$

is used to approximate the triple interactions, where $B_{kk'k''}$ are parameters, and ρ has the same numerical value as in the pairwise potential. Triplets of ions formed by two ions of the same sign and one ion of the opposite sign were taken into account in the last term in (2) in the summation over the crystal lattice. The configuration of such triplets for the NaCl lattice (under normal conditions oxides of the alkaline-earth metals have this kind of structure) is an isosceles right triangle, whose two sides equal the shortest distance R between the ions, and the third side is $\sqrt{2}R$. Experimental characteristics of the free oxides, the binding energy, the equilibrium volume [8], and the second-order elastic modulus [10-13] were used to determine the four unknown parameters of the binding energy function.

The equations of state of hydrostatic compression of oxides of the alkaline-earth metals in the B1 and B2 phases, computed on the basis of the binding energy function obtained, are in good agreement with existing experimental data [14-16]. The Gruneisen coefficients $\gamma(V)$ were calculated by the Slater–Landau (SL), Dugdale–Macdonald (DM), Zubarev–Vashchenko (ZV) formulas to compute the shock adiabats. Good agreement between the computed values $\gamma(V_0)$ and experiment for MgO is obtained in a computation using SL, and for CaO, SrO using ZV. We know of no experimental values of $\gamma(V_0)$ for BaO. The computed values of $\gamma(V_0)$ are presented in Table 1. Computation of the shock adiabats for the phase B2 was by means of (1) with parameters of the initial state of the lattice B1 with U(V), $P_x(V)$, $\gamma(V)$ referred to the phase B2. In the case of MgO the shock compression pressure $P_H(V)$ as computed by using the $\gamma(V)$ according to Slater–Landau, and according to Zubarev–Vashchenko for CaO, SrO, BaO. Computed pressures on the zero isotherm $P_x(V)$ and

Tomsk. Translated from Zhurnal Prikladnoi Mekhaniki i Tekhnicheskoi Fiziki, No. 3, pp. 132-136, May-June, 1980. Original article submitted June 5, 1979.

0021-8944/80/2103-0397$07.50

TABLE 1

Crystal	$\gamma(V_0)$			Experiment
	SL	DM	ZV	
MgO	1,58	1,25	0,92	1,54
CaO	1,78	1,45	1,12	1,19
SrO	1,79	1,46	1,13	1,11
BaO	1,87	1,54	1,21	—

TABLE 3

Crystal	Phase B1		Phase B2	
	a, km/sec	b	a, km/sec	b
MgO	7,25	1,17	5,10	1,71
CaO	6,30	1,26	4,63	1,63
SrO	3,97	1,27	2,61	1,59
BaO	2,68	1,27	2,62	1,54

TABLE 2

Crystal	Phase B1			Phase B2		
	V_0/V	P_x, kbar	P_H, kbar	V_0/V	P_x, kbar	P_H, kbar
MgO	1,17	372	376	1,61	1619	1686
	1,20	473	481	1,72	2117	2431
	1,28	708	733	1,78	2404	2904
	1,32	845	884	1,84	2720	3464
	1,51	1554	1730	1,91	3068	4133
	1,75	2603	3209	1,97	3450	4942
	1,88	3299	4378	2,04	3870	5932
CaO	1,17	310	313	1,51	866	918
	1,20	397	403	1,56	1025	1122
	1,28	604	622	1,61	1203	1359
	1,32	726	755	1,72	1620	1956
	1,42	1015	1081	1,84	2136	2773
	1,57	1586	1770	1,97	2771	3916
	1,88	3044	3866	2,04	3141	4660
SrO	1,17	233	236	1,46	540	559
	1,20	298	304	1,51	648	695
	1,28	455	469	1,61	903	1033
	1,37	651	685	1,72	1222	1490
	1,46	895	968	1,84	1615	2120
	1,68	1575	1840	1,97	2102	3005
	1,88	2309	2943	2,04	2386	3582
BaO	1,17	198	201	1,38	260	267
	1,20	254	259	1,46	408	449
	1,28	390	404	1,56	594	696
	1,37	562	596	1,67	829	1033
	1,46	779	851	1,78	1121	1502
	1,68	1391	1661	1,90	1485	2165
	1,88	2061	2726	2,04	1936	3135

the shock compression pressure $P_H(V)$ of the oxides as functions of the relative compression V_0/V are presented in Table 2. The shock adiabats of MgO, CaO, BaO are represented in Figs. 1-3 (experimental data: 1 from [17], 2 from [1], 3 from [15]). In the case of MgO and CaO the experimental points from [1, 17] are in good agreement with the computed curve of $P_H(V)$ for the B1 phase; the passage to the compact B2 phase was not established experimentally. In the case of BaO the phase transition holds in the low pressure area [3, 15]. The computed shock adiabats of the B1 and B2 lattices for BaO are close to the experimental points referring to static compression [15] in the above-mentioned domain. There are no experimental data on the shock compression of SrO in the literature. Good agreement between experiment $P_x(V)$ and $\gamma(V_0)$, as well as the utilization of the experimental characteristics of the free state in determining the binding energy function parameters, allow the hope that the computed shock adiabats for SrO would, as for MgO and CaO, describe the actual behavior of this crystal under shock compression conditions sufficiently correctly.

The shock adiabats obtained for the crystal under consideration allowed the computation of a relationship between the shock velocity D and the mass velocity u. The following relations from the conservation laws were used in the computations

$$D(v) = v_0\sqrt{P_H/(v_0 - v)}, \quad u(v) = \sqrt{P_H(v_0 - v)},$$

where P_H and v (the specific volume) are taken from our computations. The relation between D and u is interpolated in a broad range of velocities by a function of the form

$$D = a + bu. \tag{3}$$

The parameters a and b found from the computed velocities D and u by least squares are presented in Table 3 for the B1 and B2 phases of the oxides. The location of experimental points relative to the computed line (3) is shown in Fig. 4 for the crystals MgO and CaO (1 from [17], 2 from [1]). The experimental points stack up well on the computed lines (3) corresponding to the B1 phase of the oxides MgO and CaO.

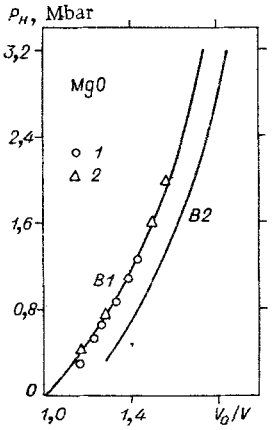

Fig. 1

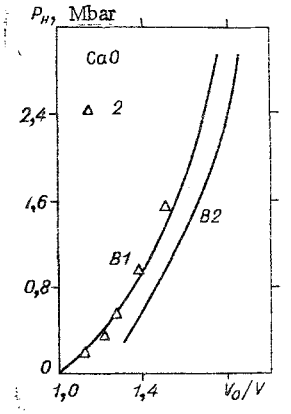

Fig. 2

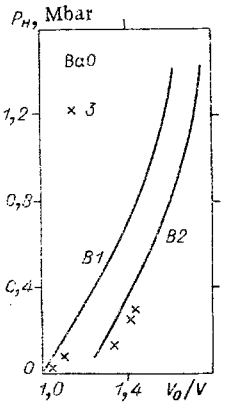

Fig. 3

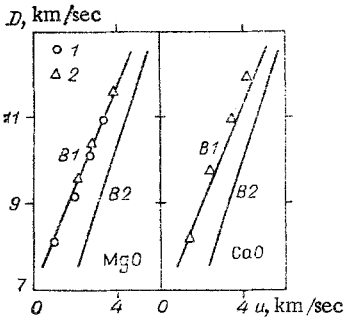

Fig. 4

The results obtained can be used in interpreting experimental results on the shock compression of oxides, as well as to construct the additive equations of state for minerals and mountain rocks.

LITERATURE CITED

1. L. V. Al'tshuler and I. I. Sharipdzhanov, "Additive equations of state of silicates under high pressures," Izv. Akad. Nauk SSSR, Fiz. Zemli, No. 3 (1971).
2. N. G. Kalashnikov, M. N. Pavlovskii, G. V. Simakov, and R. F. Trunin, "Dynamic compressibility of minerals of the calcite group," Izv. Akad. Nauk SSSR, Fiz. Zemli, No. 2 (1973).
3. L. V. Al'tshuler and I. I. Sharipdzhanov, "Crystal chemistry of the high-pressure phases of oxides and minerals," Combustion and Explosion. Materials of the Fourth All-Union Symposium on Combustion and Explosion [in Russian], Nauka, Moscow (1977).
4. L. V. Al'tshuler, M. N. Pavlovskii, A. V. Kuleshov, and G. V. Simakov, "Investigation of halides of the alkaline metals at the high pressures and temperatures of shock compression," Fiz. Tverd. Tela, 5, 279 (1963).
5. V. A. Zhdanov and V. V. Polyakov, "Shock adiabats of alkaline-halide crystals," Prikl. Mekh. Tekh. Fiz., No. 6 (1976).
6. V. N. Zharkov and V. A. Kalinin, Equations of State of Solids at High Pressures and Temperatures [in Russian], Nauka, Moscow (1968).
7. Ya. B. Zel'dovich and Yu. P. Raizer, Physics of Shock Waves and High-Temperature Hydrodynamic Phenomena [in Russian], Nauka, Moscow (1966).
8. S. Cantor, "Lattice energies of cubic alkaline-earth oxides. Affinity of oxygen for two electrons," J. Chem. Phys., 59, 5189 (1973).
9. I. P. Bazarov and V. V. Kotenok, "Theory of polymorphic transformations in ionic crystals," Zh. Fiz. Khim., 47, 2239 (1973).
10. S. Y. La and G. R. Barsch, "Pressure derivatives of second-order elastic constants of MgO," Phys. Rev. 172, 857 (1968).
11. A. J. Pointon and R. G. F. Taylor, "Elastic constants of magnesia, calcia, and spinel at 16 GHz and 4.2°K," Nature, 219, 712 (1968).
12. D. L. Johnston, P. H. Thraster, and R. J. Kearney, "Elastic constants of SrO," J. Appl. Phys., 41, 427 (1970).
13. V. H. Vetter and R. A. Bartels, "BaO single crystal elastic constants and their temperature dependence," J. Phys. Chem. Solids, 39, 1448 (1973).

14. E. A. Perez-Albuerne and H. G. Drickamer, "Effect of high pressure on the compressibilities of seven crystals having the NaCl and CsCl structures," J. Chem. Phys., 43, 1381 (1965).
15. Liu Lin-Gun and W. Basset, "Effect of pressure on the crystal structure and the lattice parameter of BaO," J. Geophys. Res., 77, 4934 (1972).
16. Liu Lin-Gun and W. Basset, "Changes of the crystal structure and the lattice parameter of SrO at high pressure," J. Geophys. Res., 78, 8470 (1973).
17. W. Mason, "Application of physical acoustics in quantum solid state physics," Physical Acoustics [Russian translation], Mir, Moscow (1970).

STRESSED STATE OF A CEMENTED POROUS MEDIUM WITH AN UNDERGROUND EXPLOSION

A. N. Bovt, V. I. Kobets, A. M. Maslennikov, E. V. Sumin, V. K. Sirotkin, V. S. Fetisov, and E. A. Shurygin

UDC 534.222

The investigation of the behavior of a cemented porous medium with an underground explosion is of considerable interest. This is connected with the fact that many rocks (e.g., gas-and-oil-saturated collectors) are cemented porous media, saturated by a gas or a liquid. At the same time, many important questions connected with the action of explosive loads on such media have been insufficiently studied. In [1, 2] a model was formulated, and experimental investigations were made of an underground explosion in soft soils. Explosion in a brittle medium was studied in [3, 4]. However, it is well known that cemented porous media differ in a number of special characteristics [5]: an increased compressibility in comparison with excavated rock, a considerable porosity (in distinction from soft soils), etc. For practical applications, an important question is that of the residual stresses, arising at the moment of the breakdown of the underground cavity, which will determine the rheological behavior of the medium in the vicinity of the explosion. The present article describes a method and the results of experimental investigations of an underground explosion in porous cement blocks.

1. Experimental explosions were carried out in cement blocks with a diameter of 790 mm and a height of 890 mm. The blocks were put into metallic casings with a wall thickness of 10 mm. The power of the explosion was selected from the condition that the time of the formation of the cavity must be less than twice the time of the passage of the wave of the compression up to the limits of the block. The experiments were made using charges of TG-20/80 with a weight of 12 g, having a cylindrical form with a height equal to their diameter. The blocks were prepared by filling metallic casings with a cement solution with VTs-0.5. Before the solution was poured, a tube was installed in the center of the vessel; when the tube was removed from the hardening solution, a hole was formed, into which the charge was lowered. The charge was installed at the center of the block and sand was poured in to a height of 40 cm. The remaining part of the charging hole was sealed by a compound based on an epoxide resin. To determine the physicomechanical properties of the medium at the moment of the explosion, samples were taken. The mean values of the properties of the medium are given in Table 1. To make dynamic measurements, before the solution was poured, wire-type strain-gauge pickups were installed radially and azimuthally with respect to the front of the wave. The overall dimensions of the pickups were: diameter 4 mm, length 10 mm. Micromodular stabilitrons were used as converters. The principle of the action of a pickup consisted in the following. The pressure is transmitted to the silicon crystal of a diode, whose sensing layer is a p–n transition. A direct current is passed through the diode from a current generator. An increase or decrease in the thickness of the p–n transition with the action of a load on the crystal brings about a change in the voltage drop at the p–n-transition, which is recorded using an amplification device. After an analysis of the oscillograms of the stresses in the compression wave, the following dependence of the maximal radial σ_{rm} and azimuthal $\sigma_{\varphi m}$ stresses on the distance were obtained

$$\sigma_{rm} = 71.4\,(W^{1/3}/r)^{2.5}, \quad \sigma_{\varphi m} = 59.7\,(W^{1/3}/r)^{2.75},$$

where W is in kg, r is in m, σ is in kg/cm^2.

Figure 1 shows a typical oscillogram of the stresses at different points from the center of the charge, where the crosses denote the residual stresses; 0 denotes zero explosion; 2φ, 5r are the number of the pickup and the recorded azimuthal components of the stresses, respectively; r is the distance from the pickup to the charge. On some oscillograms there are residual stresses differing in sign. It is well known that, with the hardening of a cement solution there arises a compressive stress, which, in the experiments, was around 200 kg/cm^2, and with respect to which the parameters of the wave were recorded. The appearance of negative stresses beyond the zone of the breakdown is explained by discharging of the pickups from the phonon pressure due to the appearance of elongational stresses in the medium.

Figures 2 and 3 show the distribution of the residual radial σ_r and azimuthal σ_φ stresses, where 1 is the measured, and 2 the reduced stress. Since the explosions took place in blocks whose yield points differed somewhat in value, on the axis of ordinates there are plotted the ratios of the actually recorded residual stresses to the crushing strength of the

Moscow. Translated from Zhurnal Prikladnoi Mekhaniki i Tekhnicheskoi Fiziki, No. 3, pp. 137-142, May-June, 1980. Original article submitted June 26, 1979.

0021-8944/80/2103-0400$07.50

TABLE 1

Density ρ, g/cm^3	1,9
Velocity of longitudinal elastic waves, km/cm	3,2
Velocity of transverse elastic waves, km/cm	1,6
Compressive strength σ^*, kg/cm^2	220
Young modulus $E \cdot 10^5$	1,51
Poisson coefficient ν	0,29
Porosity m_0, %	20

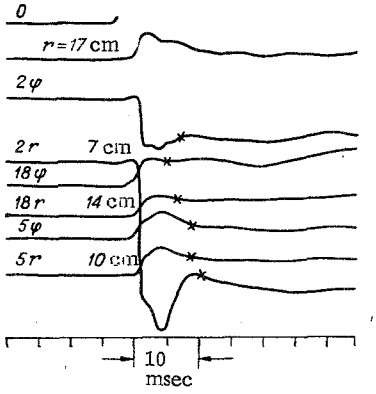

Fig. 1

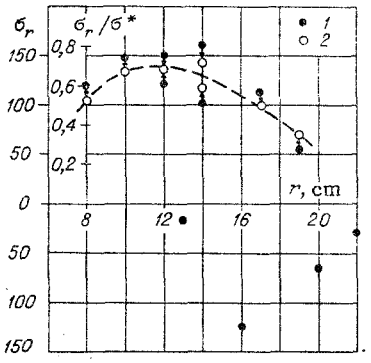

Fig. 2

samples for each experiment. It can be seen that the experimentally determined field of the residual stresses depends nonmonotonically on the distance and is characterized by the presence of a maximum. The radius of the cavity, measured in the experiments, was 2.1 times as great as the radius of the charge.

2. To bring out the principal special characteristics of the field of the residual stresses, it must be considered theoretically. First, it is expedient to examine a model problem in a simplified statement, allowing of an analytical solution.

We consider the problem of the adiabatic expansion of an underground explosion in a porous medium. We postulate that, when the shear stress $\tau = \sigma_r - \sigma_\varphi$ attains the yield point Y, there is complete closing of the pores. We assume that the condition for creep of the medium has the form $|\tau| = Y$. Behind the form of the closing of the pores, which coincides with the front of the plastic wave, the medium flows like an incompressible medium. Such a statement of the problem is analogous to that developed in [6, 7].

At early moments of time, the front of the closing of the pores coincides with the front of the shock wave. Subsequently, with a decrease in the intensity and the velocity of the shock wave, an elastic precursor breaks away ahead. We shall be interested in the stressed state in the neighborhood of the cavity at the moment of its collapse. In this case, it is possible to neglect the role of wave processes connected with the elastic compressibility of the material, both ahead of and behind the front of the closing of the pores.

Using the condition of incompressibility, the equation of continuity, and the equation of motion, we find the field of the velocities and the field of the stresses ahead of the front of the closing of the pores (i.e., in the elastic zone)

$$u = \lambda_+(t)/r^2, \quad r > R; \tag{2.1}$$

$$\sigma_r = -p_h + \frac{\rho^+}{r}\left(\dot{\lambda}_+ - \frac{\lambda_+^2}{2r^3}\right) - \frac{2}{3}Y\frac{R^3}{r^3}; \tag{2.2}$$

$$\sigma_\varphi - \sigma_r = YR^3/r^3, \tag{2.3}$$

where the condition at infinity is used $\sigma_r = \sigma_\varphi = -p_h$ (p_h is the lithostatic pressure) and at the plastic front $r = R\sigma_\varphi - \sigma_r = Y$; Y is the yield point.

In the region behind the front of the closing of the pores, the field of the velocities and the field of the stresses will be determined by the relationships

$$u = \lambda_-(t)/r^2, \quad R > r > a; \tag{2.4}$$

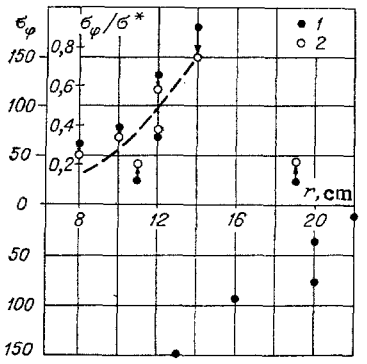

Fig. 3

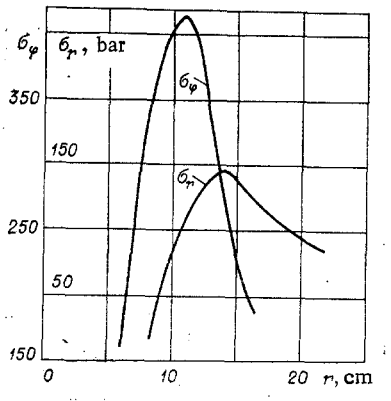

Fig. 4

$$\sigma_r = -p(a) + 2Y\ln\frac{r}{a} + \rho_+\dot{\lambda}_-\left(\frac{1}{a}-\frac{1}{r}\right) - \frac{\rho_+\lambda_-^2}{2}\left(\frac{1}{a^4}-\frac{1}{r^4}\right); \tag{2.5}$$

$$\sigma_\varphi - \sigma_r = Y, \tag{2.6}$$

where the condition at the boundary of the cavity is used $\sigma_r(a) = -p(a)$, ($p(a)$ is the pressure of the gases inside cavity of radius a).

To close the system of equations, we write the condition of joining for the velocities and stresses at the front of the closing of the pores

$$\lambda_- = (1-m)\lambda_+ + mR^3\dot{R}; \tag{2.7}$$

$$\sigma_r(R_-) - \sigma_r(R_+) = -\frac{\rho_+(1-m)}{mR^4}(\lambda_+ - \lambda_-)^2. \tag{2.8}$$

We shall consider porous media such that the porosity satisfies the condition $m \gg Y/E \sim 10^{-3}$, where E is the Young modulus. In this case, at the asymptotic limit $(a/a_0)^3 \gg l$ (a_0 is the initial radius of the charge) we obtain the following between the radius of the front of the closing of the pores R and the radius of the cavity:

$$R = am^{-1/3}. \tag{2.9}$$

At this limit we obtain the evaluation $\lambda_- \ll \lambda_+$. Then, for the radial stress in the region behind the front of the closing of the pores, using (2.2), (2.5), (2.8), (2.9), we obtain the relationship

$$-\sigma_r = -p(a) - 2Y\ln\frac{r}{a} + \frac{2Y}{1-m^{1/3}}\left[\frac{p_h - p(a)}{2Y} - \frac{1}{3}\ln m\right]\left(1-\frac{a}{r}\right).$$

It can be noted that, when the expression in square brackets is positive, the expression behaves in a nonmonotonic manner. It attains a maximum at the point

$$r_m = \frac{a}{1-m^{1/3}}\left[\frac{p_h - p(a)}{2Y} - \frac{1}{3}\ln m\right].$$

In what follows we assume that $|p_h - p(a)| \ll 2Y$ at the moment of collapse of the cavity. In this case, we obtain a simple expression for the radius of the maximal stress

$$r_m = \frac{1}{3}\frac{a}{1-m^{1/3}}\ln\frac{1}{m}. \tag{2.10}$$

With reasonable values of the porosity, the radius of the zone of maximal stresses will be less than the radius of the zone of plastic flow.

Thus, the residual stresses will behave in a nonmonotonic manner. As an analysis shows, this monotonicity is connected in the present case with the competition between the static and dynamic terms in expression (2.5). The static term prevents the expansion of the cavity, and therefore falls with the distance. The dynamic term is connected with the acceleration of the medium, directed toward the cavity, which leads to a deceleration of the medium and to its stopping. It must be noted that the evaluations for the radius of the zone of plastic flow (2.9) and the zones of increased stress (2.10) are lower evaluations, since, with their derivation, it was assumed that, at the front, there is irreversible closing of all the pores.

3. Taking account of the role of wave processes connected with the elastic compressibility of the substance, the study of the gas-saturated pores, closed in the loading wave, requires the solution of a complete system of equations of hydrodynamics in partial derivatives, which is possible only by numerical methods. The numerical calculations were made

using a model of an elasticoplastic porous gas-saturated medium. It is assumed that the motion of the medium is spherically symmetrical. The principal equations describing the spherically symmetrical motion of the medium in Lagrangian coordinates for this model have the form

$$\frac{\partial v}{\partial t} = v\left(\frac{\partial u}{\partial r} + 2\frac{u}{r}\right), \quad \frac{\partial u}{\partial t} = v\left(\frac{\partial \sigma_r}{\partial r} + 2\frac{\tau}{r}\right),$$
$$\frac{\partial e}{\partial t} + p\frac{\partial v}{\partial t} = \frac{2}{3}\tau v\left(\frac{\partial u}{\partial r} - \frac{u}{r}\right), \tag{3.1}$$

where v and e are the specific volume and the specific energy of the medium as a whole; u is the velocity; $\tau = \sigma_r - \sigma_\varphi$; σ_r and σ_φ are the radial and tangential components of the stress tensor; $p = -(1/3)(\sigma_r + 2\sigma_\varphi)$; r is an Euler coordinate. The tensor of the stresses, σ_{ij}, denoting the total stress applied to the porous medium can be connected with the stress $\sigma_{ij}^{(1)}$, acting in the solid component, and the pressure p_1 of the gas, filling the pores [8]:

$$\sigma_{ij} = (1-m)\sigma_{ij}^{(1)} - mp_1\delta_{ij} \tag{3.2}$$

(m is the porosity).

We further postulate that $\sigma_{ij}^{(1)} = -3p_1$, i.e., the equality of the pressures in the skeleton and of the gas in the pores. A similar postulation is valid, generally speaking, with sufficiently high pressures (~10 kbar); however, to simplify the calculations, we shall assume that the pressures in the components making up the porous material are identical.

The system of equations (3.1) is closed by the elasticoplastic equations of state. In the elastic zone, the substance is deformed in accordance with Hooke's law

$$d\tau/dt = 2G(du/dr - u/r). \tag{3.3}$$

(G is the shear modulus). In the plastic region, the condition for creep has the form

$$|\tau| = \sigma^*. \tag{3.4}$$

To take account of the gas saturation of the porous medium, a method analogous to [9] is used. In this case, the total specific volume v and the total specific energy were calculated using the formulas

$$v = R_1v_1 + R_2v_2, \; e = R_1e_1 + R_2e_2$$

(1 denotes the solid component, 2 the gas). Here R_i is the weight content of a component, connected with the porosity; v_i and e_i are the specific volume and the specific energy of the corresponding component. The equation of state of the solid component had a Mie–Gruneisen form [10]. For the gas, the equation of state of an ideal gas with $\gamma = 1.4$ was used.

At the initial moment of time, the pressure and the density of the explosion products were given in a region whose size coincides with the radius of the charge. The radius of the charge was calculated from experimental data, in accordance with its weight. The system of equations (3.1)-(3.4) was solved numerically in a computer using the mechanical parameters of the medium in which the experiment was made.

Numerical solution of the system of equations (3.1) gives the following picture of the formation of the zone of contraction around the cavity. In the stage of the expansion of the original gas cavity, the medium around it is brought into motion. After the cavity has attained a maximal radius, a rotational motion starts. This starts as a result of the fact that, in some intermediate region between the boundary of the cavity and the shock wave, the mass velocity of the medium becomes equal to zero, and then negative, i.e., as a result of unloading, the medium starts to move toward the center. As a result of this kind of contrary motion, there is a certain densification of the medium in the vicinity of the cavity. When the back motion reaches the boundary of the cavity, the medium around it starts to flow first elastically, and then plastically toward the center. The presence of a zone of plastic flow at the boundary of the cavity leads to a further rise in the stresses in the medium surrounding the cavity. As a result, in the neighborhood of the cavity there arises a characteristic zone of a nonmonotonic distribution of σ_r and σ_φ. The value of the maximum in Fig. 4 depends on the porosity of the medium and decreases with an increase in the latter. Qualitatively, the form of the dependence of σ_r and σ_φ on the distance coincides with analytical evaluations and with the experimental data in Figs. 2 and 3. It must be noted that the residual stresses in the calculations of [1] had an analogous nonmonotonic character. However, in this work, the character of the residual stresses and their formation were not discussed, since the main stress in the work was laid on the dynamic development of an explosion in a saturated porous medium.

LITERATURE CITED

1. V. D. Alekseenko, S. S. Grigoryan, A. F. Novgorodov, and G. V. Rykov, "Experimental investigations of the dynamics of soft soils," Dokl. Akad. Nauk SSSR, 133, No. 6 (1960).
2. S. S. Grigoryan, "Solution of the problem of an underground explosion in soft soils," Prikl. Mat. Mekh., 28, No. 6 (1964).
3. V. M. Tsvetkov, I. A. Sizov, and A. D. Polikarpov, "The behavior of a brittle-fracturing medium with an underground explosion," FTPRPI, No. 4 (1977).

4. V. M. Tsvetkov, I. A. Sizov, and N. M. Syrnikov, "The mechanism of the fracture of a brittle medium with an underground explosion," FTPRPI, No. 6 (1977).
5. The Physics of Explosion [in Russian], Nauka, Moscow (1975).
6. A. S. Kompaneets, "Shock waves in a plastic densifying medium," Dokl. Akad. Nauk SSSR, 109, No. 1 (1956).
7. E. I. Andriankin and V. P. Koryavov, "A shock wave in an alternately densified plastic medium," Dokl. Akad. Nauk SSSR, 128, No. 2 (1959).
8. V. N. Nikolaevskii, K. S. Basinev, A. T. Gorbunov, and G. A. Zotov, The Mechanics of Saturated Porous Medium [in Russian], Izd. Nedra, Moscow (1974).
9. G. M. Lyakhov, Principles of the Dynamics of Explosion Waves in Soils and Rocks [in Russian], Nedra, Moscow (1974).
10. Ya. B. Zel'dovich and Yu. P. Raizer, Physics of Shock Waves and High-Temperature Hydrodynamic Phenomena [in Russian], Izd. Fizmatgiz, Moscow (1963).
11. E. E. Lovetskii, A. M. Maslennikov, and V. S. Fetisov, "Expansion of a gas cavity in a gas-saturated elastoplastic medium," Zh. Prikl. Mekh. Tekh. Fiz., No. 1 (1979).

KINETIC MODEL OF SPALLING FRACTURE

B. G. Kholodar'

UDC 539.4.019+620.187.7

The theory of longevity based on thermofluctuational representations [1] has received considerable development at this time. It is shown that the thermofluctuational mechanism of fracture is conserved in a longevity time band from several years to fractions of a microsecond.

The S. N. Zhurkov formula

$$t_p = t_0 \exp\left\{\frac{U_0 - \alpha\sigma}{k\vartheta}\right\} \tag{1}$$

is a classical dependence of the longevity t_p on the load, where $t_0 \approx 10^{-13}$ sec, k is the Boltzmann constant, ϑ is the absolute temperature, σ is the tensile stress, U_0 is the activation energy of the fracture process, and α is a structural parameter of the material.

However, the possibilities of practical application of (1) are limited because the parameters U_0 and α turn out to be dependent on the loading conditions (the kind of stress state, the loading mode, etc.). These limitations can be reduced to a significant degree if, as is customary in mechanics [2, 3], differential equations for the development of vulnerability, particularly those that would yield a dependence close to the S. N. Zhurkov formula for the longevity as solutions for the case of one-dimensional tension on a rod, were used to perform the computations.

Equations of a similar kind were proposed in [4, 5] for the one-dimensional and volume states of stress. Comparing the computation results with experimental data shows that the equations yield the regularities of the development of material vulnerability sufficiently completely in different loading modes.

In the interests of simplification, the one-dimensional case is examined in this paper, and the equation

$$d\omega/d\tau = (1 - \omega)Sh\{\varphi(X/(1 - \omega))\} \tag{2}$$

is used to perform the computations, where ω is the material vulnerability ($0 \leqslant \omega \leqslant 1$); τ is the dimensionless time introduced in place of the time t by using the formula $\tau = \nu t$; $\nu = \nu_0 e^{-Y}$; $Y = U_0/k\vartheta$; ν_0 is a material constant; $X = \alpha\sigma/k\vartheta$ is a dimensionless load parameter; and U_0, α, k, ϑ, σ retain the same meanings as in (1).

The factor $(1 - \omega)^{-1}$ in the argument of the function φ takes account of the rise in the mean stresses in the damaged section.

In conformity with the general representations [1], we assume the activation energy U of the fracture processes to vary nonlinearly as a function of the applied stress σ. The general view of the dependence $U(\sigma)$ and its approximation by piecewise-linear functions are shown in Fig. 1.

In performing the computations below, we used the dependence $\varphi(X/(1 - \omega))$ that describes the reduction of the activation energy of the fracture processes $U = U_0 - \varphi(\sigma)$ from its initial value U_0 in the form of a piecewise-linear function "without strengthening," which recalls the strain diagram of an ideally plastic material in its form:

Chelyabinsk. Translated from Zhurnal Prikladnoi Mekhaniki i Tekhnicheskoi Fiziki, No. 3, pp. 142-148, May-June, 1980. Original article submitted May 21, 1979.

0021-8944/80/2103-0404$07.50